Materials Advances

ROYAL SOCIETY OF CHEMISTRY

PAPER

View Article Online
View Journal | View Issue

Cite this: *Mater. Adv.*, 2025, 6, 3084

Dual alkali etching for osseointegration and reduced bacterial adhesion: a feasible alternative to SLA

Sushmita Chettri,[ab] Huasi Zhou,[a] Wei Zhu,[c] Håkan Engqvist,[a] Deepa Seetharaman *[b] and Wei Xia *[a]

Received 10th December 2024,
Accepted 23rd March 2025

DOI: 10.1039/d4ma01223b

rsc.li/materials-advances

Titanium and its alloys stand out as the preferred materials for crafting implant prostheses. However, there exists a need to enhance the surface physicochemical properties of titanium alloys to optimize their surface activity as implant materials. While various surface modification techniques demand intricate and costly infrastructure, our study introduces a simple solution – a straightforward dual alkali treatment for titanium alloys. This approach aimed to establish a simple method for achieving osseointegration while also enhancing the bacteriostatic nature of the material. In our investigation, Ti-6Al-4V samples were subject to sequential treatment with NH_4OH and NaOH for 24 hours at room temperature and *vice versa*. Subsequent analyses employing XRD, SEM, XPS, and optical profilometry, were performed to examine the effect of the treatment on the morphology and phase composition of the treated samples. The modified samples exhibited satisfactory bioactivity coupled with enhanced bacteriostatic behavior.

1. Introduction

Dental implants have become a *sine qua non* for the replacement of lost teeth and restoration of the chewing function and aesthetic appearance. Titanium is considered the gold standard for dental implants owing to its presence and usage in dentistry for 6–7 decades.[1,2] Titanium and its alloys are known for their suitable mechanical and biocompatible properties in the implant industry. However, the low bioactivity of titanium poses a limitation in osseointegration. Many studies have therefore attempted to improve the biointegration of titanium implants by modifying their surface.

Research has demonstrated that the physical topography, chemical composition, and wettability of the implant surface, play a key role in its ability to integrate into the host tissue/bone. Several physical surface modification techniques have been developed and used in commercial implants, the most popular being sandblasting, grit blasting, acid-etching, plasma spraying, anodization and laser ablation.[3] Additionally, SLA is one of the successful surfaces in clinical implant dentistry with a 10-year survival rate reported to be 95–97%.[4] Although SLA is a satisfactory surface treatment, there is a search for a technique that encourages stable and early osseointegration. Similarly, anodic oxidation of the implant surface has revealed clinical long-term survival and success rate.[5] Plasma spray coatings of hydroxyapatite (HAP) on titanium implant surfaces are commonly used, as they demonstrate excellent biocompatibility with good mechanical properties. However, many concerns have been raised regarding the stability of these coatings. High porosity and amorphous content weaken the coating and affect bone-implant integration. Moreover, the disintegration of coatings may cause inflammation around the implant.[6] Thermochemical treatments, with acid, base, or a combination of both, have also proved to activate osseointegrative Ti surfaces, which are otherwise bioinert.[7,8]

The colonization and proliferation of bacteria that form a biofilm on the implant surface can result in peri-implantitis – a gum-associated disease that leads to inflammation and bone loss. Microbial adhesion is tackled by designing the implant's surface to inhibit biofilm formation. Grafting of antibacterial peptides and coating with a drug-releasing antibacterial agent or anti-adhesive polymer surface are some of the strategies adopted.[2] However, the loss of the coated material in the long term is always a concern. Furthermore, the equipment associated with techniques such as plasma spraying and laser ablation, involve significant cost and infrastructure.

Dental implants have a clinical success rate of around 90% over a 10–15 year implantation period.[9] The associated failure could be mainly attributed to microbial adhesion and

[a] *Applied Materials Science, Department of Materials Science and Engineering, Uppsala University, Uppsala, Sweden. E-mail: Wei.Xia@angstrom.uu.se*
[b] *Department of Physics, Sri Sathya Sai Institute of Higher Learning, Andhra Pradesh, India. E-mail: deepaseetharaman@sssihl.edu.in*
[c] *Department of Orthopedics, Peking Union Medical College Hospital, Chinese Academy of Medical Sciences & Peking Union Medical College, Beijing, China*

insufficient bone-promoting characteristics.[10] Surface modification strategies that focus on one of the above issues are therefore insufficient and do not guarantee implant success. Hence, it is imperative to develop a simple and cost-effective surface modification technique that simultaneously improves osseointegration and minimizes the risk of peri-implant complications, while ensuring swift and assured healing.

In this study, dual alkaline etching has been performed to investigate the effect of the alkaline solutions on the bioactivity and bacteriostatic behaviour of Ti and its alloy. Alkali treatment of Ti alloy with NaOH followed by heating at high temperature, or alkaline etching of the alloy at temperatures higher than room temperature has been well studied earlier.[11–14] Though these studies have shown good results, they involve subjecting the material to high temperatures, which may result in changes in its intrinsic properties. Alkali treatments have been performed predominantly using NaOH solution or combining it with H_2O_2.[15] The present study highlights the potential of room temperature alkaline etching on the surface of Grade 5 titanium alloy. Furthermore, the study examines the effect of sequential etching with combination of NaOH and another less explored alkali, NH_4OH. The aim of the study is to demonstrate a successful room temperature protocol that can be easily performed in a clinical environment before implantation. Thus, the study brings a simple and cost-efficient surface treatment strategy and its role in improving bioactivity and bacteriostatic behavior on the modified Ti alloy surface.

2. Materials and methods

2.1. Materials

Grade 5 titanium (Ti-6Al-4V) plates, having a diameter of 10 mm and a thickness of 0.5 mm, were used for this study. 5 M and 10 M NaOH (extremely pure, 98–100.5% pellets from Sigma-Aldrich) and NH_4OH (ACS reagent, 28–30% NH_3 basis from Sigma Aldrich) solutions were selected as the alkaline solutions for the chemical treatment of the Ti-6Al-4V samples. Additionally, Ti-6Al-4V mini-implant screws of length = 3.1 mm and diameter = 1.4 mm (Fig. 1) were used for the *in vivo* study.

2.2. Dual alkaline etching (DAE)

DAE was performed to investigate the effect of the double alkaline solution on the bioactivity and bacteriostatic behaviour of Ti-6Al-4V. The as-received Ti plates were thoroughly washed and ultrasonicated with 20 ml of acetone, ethanol (95%), and deionized water for 15 min each. Pre-treatment cleaning was performed to ensure the removal of the surface impurities on the Ti samples. The cleaned plates were then dried at 100 °C for 30 min. The chemical etching was done in two different sequences for each set of samples. The first set of samples (named NaN) were soaked in 10 ml of NaOH followed by 10 ml of NH_4OH for 24 h each. It was made sure that the surfaces of the samples are completely immersed in the solution. The soaking sequence was reversed for the second set (NNa).

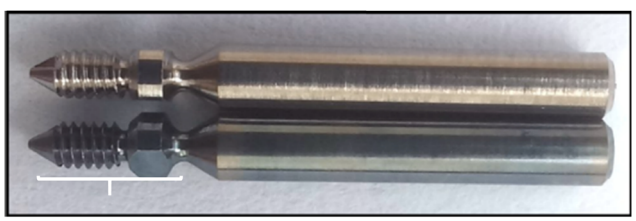

Fig. 1 Image of the untreated (top) and dual alkaline treated (bottom) mini-implants having dimensions 3.1 mm length and 1.4 mm diameter. The marked portion indicates the implant region.

Table 1 Summary of the treatment sequence for dual alkaline etching of Ti plates

Soaking time (h)	Alkali concentration (M)	Step 1	Step 2	Sample name
24	5	NaOH	NH_4OH	NaN5
		NH_4OH	NaOH	NNa5
	10	NaOH	NH_4OH	NaN10
		NH_4OH	NaOH	NNa10

The soaking process was performed with two different concentrations of the alkalis, as summarized in Table 1. After soaking for 24 h, each plate was gently cleaned with 20 ml of deionized water to wash off the excess chemical residue. Necessary caution was taken not to rub away any chemical compounds that may have formed on the Ti surface. The same procedure was adopted for the implants to examine the *in vivo* ability of the DAE surface treatment.

2.3. Material characterization

Optical profilometry (ZYGO, Middlefield, CT, USA) was performed to investigate the effect of the dual alkaline treatment on the nano/micro scale surface roughness of the samples. A vertical scanning interferometry mode was considered with 10× magnification to scan a square area of 2.1 mm^2. Each sample was subjected to five measurements, and three samples were tested in each experimental group. The video-based optical contact angle measuring system (OCA 25, Data-physics Instruments GmbH, Germany) was used to obtain the contact angle of distilled water on the samples. The angle measurement was made using ImageJ software.

An X-ray diffractometer (Siemens, Diffractometer D5000, Cu K_α X-ray source, λ = 1.54 Å, Germany) was used to examine the surface phase composition of the treated samples in a parallel beam geometry. Grazing incidence X-ray diffractometry was employed at an incidence angle of 5° and a step size of 0.02°. The scanning procedure encompassed the 2θ range from 10° to 80°, with each step lasting 3 s.

The effect of the chemical treatment on the surface morphology of the treated samples was assessed using scanning electron microscopy (SEM) (Merlin, Zeiss, Germany). The measurements were conducted at 10 nA and 5 kV for each sample. For elemental analysis, X-ray photoelectron spectroscopy (XPS) (Physical Electronics Quantum 2000, Al K_α X-ray source, USA) was used. Spectral energy calibration was performed by setting the binding energy of C–C at 284.8 eV, referred to as

adventitious surface carbon. The surface chemistry and electronic states of the chemical species in the obtained spectra were analyzed using CasaXPS software (Physical Electronics).

2.4. Colony forming unit assay

2.4.1. Bacterial culture. In this study, Gram-positive bacteria, *Staphylococcus aureus*, were used. A volume of 10 μl of this bacterial strain was streaked onto an LB agar plate and left to incubate overnight at 37 °C. Subsequently, a single fresh colony was extracted from the agar plate and introduced into 25 ml of lysogeny (Luria) broth (LB). The bacterial suspension was then subjected to a 16-hour incubation at 37 °C. Following this, the suspension underwent centrifugation at 1500 rpm for 5 min to isolate the bacteria. The isolated bacteria were re-suspended in 25 ml of fresh LB broth. The bacterial culture was further diluted to an OD_{600} of 0.2 using an OD600 DiluPhotometer (Implen, Germany).

2.4.2. Bacterial attachment assay. Each sample was thoroughly sterilized using 10 ml of 75% ethanol and meticulously positioned on a sterilized 24-well culture plate. The surfaces of the sterile samples were seeded with 15 μl of the bacterial suspension. The remaining empty wells were filled with 500 μl of phosphate buffer solution (PBS) and the entire culture plate was placed in a water bath to prevent dehydration of the bacterial suspension seeded on the samples. It was then incubated at 37 °C for 1.5 hours to facilitate the interaction between the bacteria and samples. After incubation, each sample was transferred to a tube containing 1 ml of PBS (Sigma Aldrich). The tubes were then vortexed for 1 minute to detach and re-suspend the adhered bacteria in the PBS solution. This solution was subjected to a tenfold dilution in four steps, with 100 μl taken from each dilution and placed on LB agar plates. The agar plates were then incubated overnight to allow the growth of bacterial colonies, which were subsequently counted.

2.5. Immersion test in simulated body fluid (SBF)

The titanium samples from each group were immersed in simulated body fluid (SBF) for 7 days, to mimic the early-stage bone bonding environment around the implant site. SBF was regularly replenished every two days. Utilizing SBF for material bioactivity assessment has been well-established in various studies.[16,17] After the immersion, samples were extracted from the solution, rinsed with distilled water, and carefully dried. Subsequently, SEM was employed for a comprehensive examination of the samples to assess the extent of apatite formation.

2.6. *In vivo* animal model

Twelve male Sprague–Dawley rats (340–360 g), fed on a standard diet of pellets and water, were anaesthetized using a Univentor 400 anaesthesia unit (Univentor; Zejtun, Malta) under isoflurane inhalation. Anaesthesia was maintained by continuous administration of isoflurane *via* a mask. Each rat received analgesic subcutaneously before the implantation, and daily postoperatively. After shaving and cleaning (5 mg ml^{-1} chlorhexidine in 70% ethanol), the medial aspect of the proximal tibial metaphysis was exposed through an anteromedial skin incision, followed by skin and periosteum reflection with a blunt instrument. After bone preparation with 1.4 mm and 1.8 mm diameter burrs under profuse irrigation with 0.9% NaCl, two implants from implant group NNa5, were inserted in each animal (one implant/tibia) with a hexagonal screwdriver. The locations of the implants were decided using a predetermined schedule, ensuring alternation between legs and sites. The subcutaneous layer of the wound was closed with resorbable polyglactin sutures, and the skin was closed with transcutaneously placed nylon sutures. The retrieval procedure was done after 7 and 28 days, when the rats were sacrificed by an intraperitoneal overdose of sodium pentobarbital (60 mg ml^{-1}) under anaesthesia, with 0.5 ml of a mixture of pentobarbital (60 mg ml^{-1}), NaCl and diazepam (1 : 1 : 2), and were subsequently cleaned with 5 mg ml^{-1} chlorhexidine in 70% ethanol.

The samples were scanned using a vivaCT 80 micro-CT system (SCANCO Medical AG, Bassersdorf, Switzerland) at a 12 μm resolution, applying an appropriate constrained Gaussian filter to partially suppress noise. The acquired images were reconstructed using CTAn software. Histomorphometric analysis, including the bone volume to total volume (BV/TV) ratio was conducted using CTAn software (gray value: 41000). The animal experiments in this study were approved by the Ethical Inspection Committee of Peking Union Medical College Hospital (XHDW-2015-0034).

2.7. Statistical analysis:

The statistical analysis of the bacteriostatic effect of the surface treatment was evaluated by one-way ANOVA using Prism software (GraphPad Prism Software Version 10, USA). A p-value of <0.05 was used to determine the significant difference; refer to Fig. 10a and b, where (*) implies $p < 0.05$, and (ns) implies $p > 0.05$.

3. Results and discussion

3.1. Surface profilometry

Fig. 2 shows the surface profilometry of the control (untreated) and the treated samples. The average surface roughness (S_a: arithmetic mean of the surface points from the mean plane) of the untreated samples was 0.4 μm. The images (Fig. 2(b–e)) indicate an increase in the S_a value of the chemically treated samples compared to the control. The treatment resulted in S_a values of 0.5 to 0.6 μm, with the NNa5 (Fig. 2(b)) combination having the highest average S_a = 0.56 μm, followed by NNa10, which had an average S_a = 0.52 μm.

Fig. 3(a–e) shows the difference between water contact angles for untreated and treated samples. The NNa5 and NNa10 surfaces exhibited lower contact angle compared to other test groups. This is in line with the magnitude of the observed surface roughness for NNa5 and NNa10. The increase in surface roughness could be attributed to the formation of a nanoporous network structure on the Ti surface after the wet etching.[18] The SEM images (Fig. 6(c–j)) also indicate the formation of such networks (discussed in Section 3.3). However,

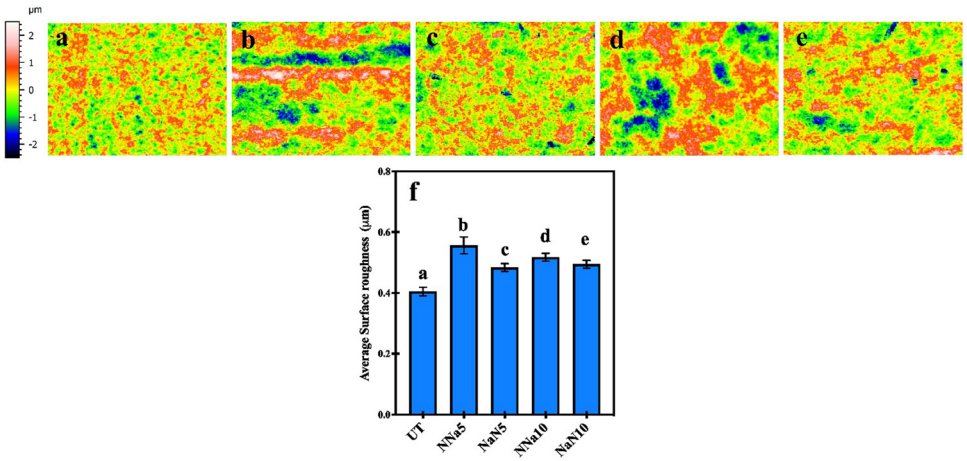

Fig. 2 (a)–(e) Results of optical profilometry measurements of the samples – difference in surface topography is indicated by the color scale; (a) untreated, (b) NNa5, (c) NaN5, (d) NNa10 and (e) NaN10; (f) comparison of average surface roughness before and after the dual alkaline etching.

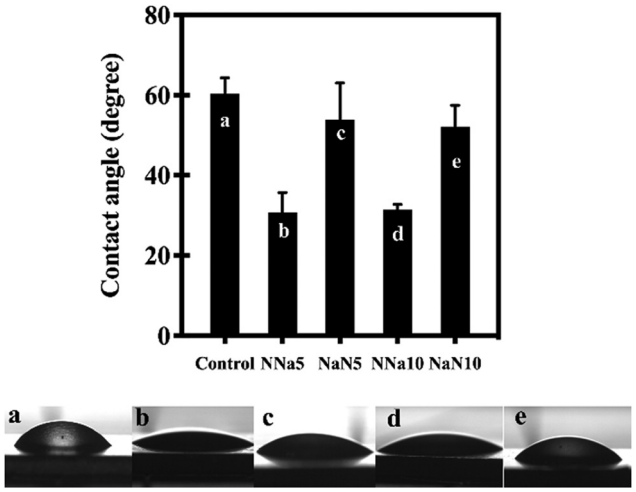

Fig. 3 Plot of water contact angles of the untreated and treated samples; (a) untreated (control), (b) NNa5, (c) NaN5, (d) NNa10 and (e) NaN10.

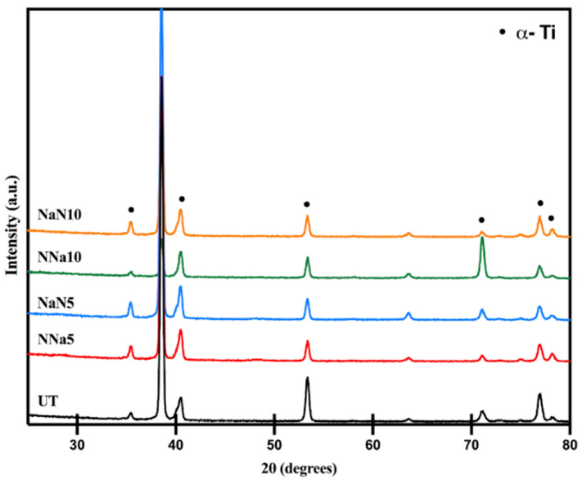

Fig. 4 GIXRD pattern of the dual alkali treated groups and the untreated samples at room temperature.

increasing the molarity of NaOH did not make a significant difference in the average roughness value. The nanoscale surface roughness has been identified as a significant factor affecting the bacterial adhesion to the substrate.[19]

3.2. Surface chemical composition

Fig. 4 shows the XRD patterns of the samples soaked in the dual alkali solutions at room temperature. The diffraction patterns of the treated samples were similar to the untreated Ti-6Al-4V discs; the resulting peaks were fitted to the reported hexagonal close-packed α-Ti (JCPDS file #44-1294).[20] However, the treated samples show an intensity reduction of the peaks at 53.3° (102) and also at 76.8° (112). According to previous research, this could be attributed to the formation of amorphous sodium titanate hydrogel, a porous structure, on the surface of the substrate.[21,22]

Fig. 5 depicts the XPS characterizations of the control and the treated samples. The survey spectra of one of the treated surfaces (NNa5) in Fig. 5b, consists of the representative peaks of Ti 2p, Ti 1s, Na 2p, N 1s, C 1s, and O 1s, indicating the influence of DAE on modifying surface chemistry post treatment. The high-resolution spectra of N 1s could be deconvolved into two sub-peaks between energy levels 394–408 eV. These sub-peaks could be designated to N–H and N–O bonds.[23–26] NNa10 samples showed a higher proportion of 84% of N–O bonds and 17% of N–H bonds. On the contrary, NaN10 samples indicated 18% of N–O and 82% of N–H. In the samples NNa5 and NaN5, the proportion of N–H bonds was found to be 75% and 63%, respectively. The fraction of N–O bonds was 25% and 38% for these groups, respectively.

3.3. Surface morphology and apatite formation

The SEM images of the untreated and 24 h dual alkaline etched Ti-6Al-4V samples are presented in Fig. 6. As compared to the unetched samples, which appear to be smooth (Fig. 6(a and b)), the etched surfaces show a change in surface morphology,

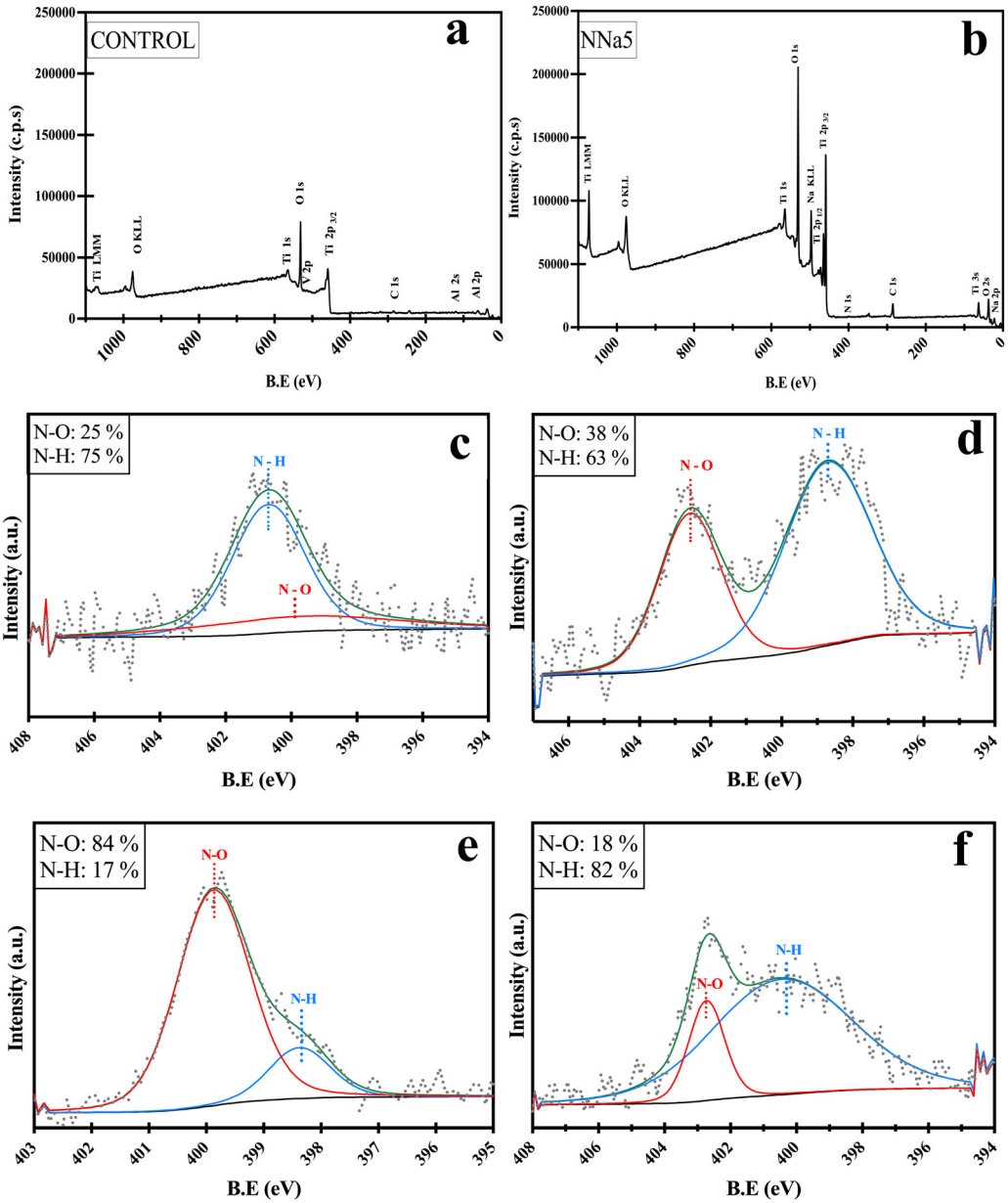

Fig. 5 XPS survey spectrum of (a) control and (b) NNa5 sample; (c)–(f) spectra of the treated samples around the 400 keV region indicating the presence of nitrogen in NO and NH bonds: (c) NNa5, (d) NaN5, (e) NNa10 and (f) NaN10.

exhibiting the formation of porous network-like structures as a result of the alkali treatment. Fig. 6(c–j) shows that the porous network formation occurred in both NaN and NNa etched samples, for both molarities of the NaOH solution.

The SEM images in Fig. 7 were taken to study the apatite formation on the control and treated samples after a week's immersion in SBF. The nucleation of nanospherical particles has been observed on the surface of all the treated samples. The apatite formation may be accelerated by the formation of titanate layers on the surface of the sample after alkali treatment with NaOH and NH_4OH.[22] The Ti-6Al-4V samples when immersed in alkaline solution form negatively charged $HTiO_3^-\cdot nH_2O$ ions.[27] These ions incorporate Na^+ and NH_4^+ ions to form an alkali titanate layer. The thickness of the layer might depend on the concentration of the alkaline solution, treatment time, and temperature.[27–29] When the alkaline-treated Ti-6Al-4V samples are soaked in SBF, the Na^+ and NH_4^+ ions are released from its alkali titanate layer into the SBF solution *via* H_3O^+ ion exchange forming Ti–OH groups on its surface.[14,30] These Ti–OH groups encourage apatite nucleation; the thicker the titanate layer, the greater the release of Na^+ and NH_4^+ ions. The samples showed no difference in the amount of apatite formation with change in molarity of NaOH. No apatite formation was observed in the control in one week's time as seen in Fig. 7(a and b). Fig. 8 depicts the titanate formation during DAE and the chemical processes schematically.

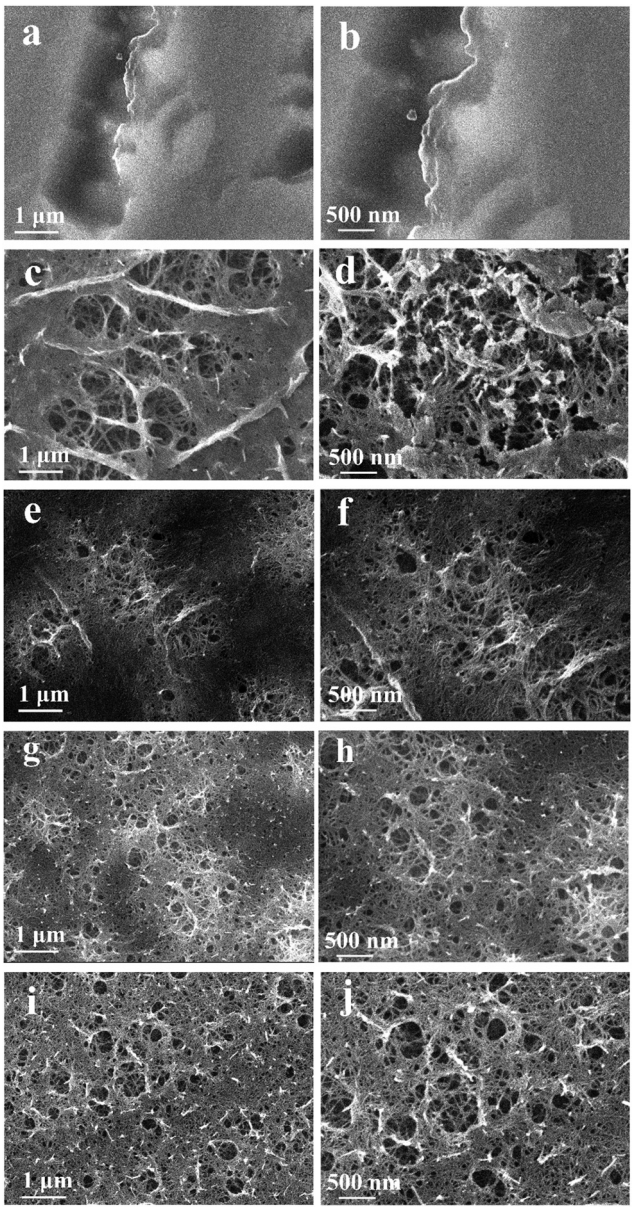

Fig. 6 SEM images of the samples taken using the in-lens detector after dual alkaline etching for 24 h; (a) and (b) untreated sample; (c) and (d) NNa5; (e) and (f) NaN5; (g) and (h) NNa10 and (i) and (j) NaN10.

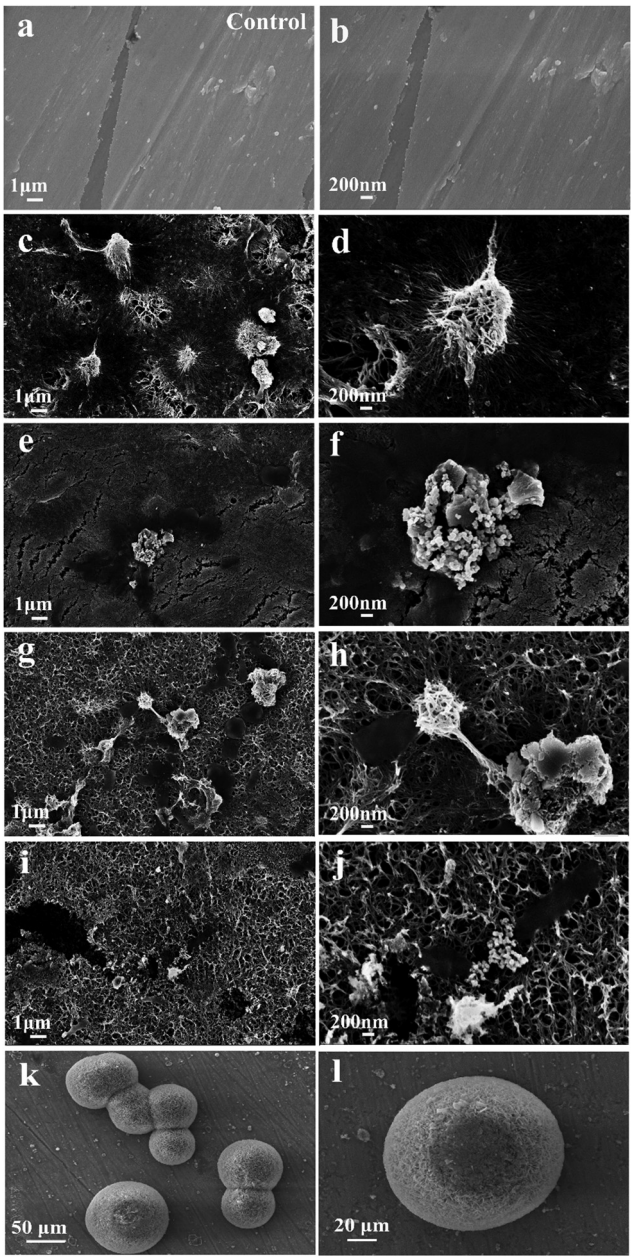

Fig. 7 SEM images of the control and the treated samples taken using the in-lens detector after immersion in SBF solution for 1 week: (a) and (b) control; the treated surfaces show the nucleation of apatite (c) and (d) NNa5; (e) and (f) NaN5; (g) and (h) NNa10; (i) and (j) NaN10; (k) and (l) low magnification, large apatite formation on the surface of NaN5 and NNa10.

3.4. DAE-modified bacteriostatic effect on Ti-6Al-4V

Peri-implantitis is a complex inflammatory condition hindering osseointegration post implantation, causing delayed healing, bone loss, and even implant failure. *S. aureus* is one of the predominant bacteria that causes peri-implantitis.[31–33] Hence, in this preliminary stage of the study, the focus was on the inhibition efficacy of the treated surface against *S. aureus*.

The bacteriostatic behaviour of the treated surfaces was evaluated using colony forming units (CFU) counting after incubation with *S. aureus*. Fig. 9 shows the viable colony-forming units on agar plates seeded with *S. aureus* after 1.5 hours of *in vitro* incubation. The untreated Ti-6Al-4V was considered as the control. Fig. 10a shows the average CFU per ml^{-1} ($\times 10^5$) of the DAE treated samples in comparison with the control. It could be observed that the DAE samples show improved bacterial inhibition compared to the control. Fig. 10a also indicates that the NNa5 samples show the best bacteriostatic ability against *S. aureus* among all the considered groups. The control was highly colonized, almost 7 times more than the treated samples, as seen in Fig. 10a. Fig. 10b shows the inhibition efficiency (%) of the treated samples with respect to the control. NNa5 shows 90% inhibition efficiency compared to the control, followed by NaN10 (82%), NNa10 (74%) and NaN5 (73%). Fig. 10(c and d) shows the SEM image of *S. aureus*

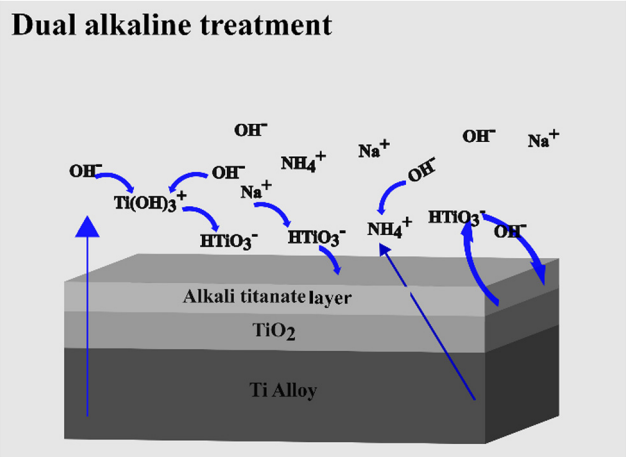

Fig. 8 Schematic representation of titanate formation and presence of ionic species as a result of dual alkaline treatment.

on the control and NNa5 after the bacterial contact for 1.5 h. The number of colonies in the control is much more than that in NNa5 implying that the bacterial adhesion is not favourable on the morphology achieved through the dual alkaline etching.

Several factors such as surface chemistry, morphology, wettability, *etc.*, contribute to the bacteriostatic behaviour of a biomaterial. Previous studies have shown that the reactive nitrogen species (RNS), in contact with the bacterial cell, exhibits a crucial role in destroying the bacterial membranes by penetrating them and destroying the proteins essential for their survival.[34]

In this study, the antibacterial effect may be attributed to the presence of RNS, such as nitrides (NO, N_2O) and amorphous oxynitride (NO_2^-).[35] The XPS analysis confirmed the presence of nitrogen on all the treated samples, though in a low amount (Fig. 5). Hence, it could be deduced that the treated samples may release active RNS when in contact with body fluids. The DAE-treated samples have also shown differences in the chemical composition (Fig. 5) and morphology (Fig. 6) and water contact angles (Fig. 3). Additionally, surface charge also affects the antimicrobial activity by inducing repulsive interaction to the bacterial cell. As the bacteria acquires negative charge in the biological environment, there will be a repulsive interaction between the bacterial cell and the surface, if the surface also acquires a negative charge.[36] Furthermore, the isoelectric point (IEP) of Ti-6Al-4V oxide is found to be ~4.4.[37] Hence, it could be implied that the treated substrate may also exhibit a negative charge in the physiological environment resulting in some degree of repulsion towards the bacterial cells. This result can also be correlated with the formation of nanometric surface roughness of the samples after alkaline treatment. Prior studies show that increase in nanometric roughness also inhibits bacterial adhesion.[38]

3.5. *In vivo* study of bone-implant formation

A preliminary *in vivo* test was conducted on Sprague–Dawley rats to study the early onset of osseointegration. The ratio of bone volume to total volume (BV/TV) was evaluated after one week and four weeks of implantation. The BV/TV ratio is a vital metric in assessing implant stability, predicting its functionality under load, and its long-term success. Fig. 11a shows the micro-CT images conducted after 1 week and 4 weeks of *in vivo* study for NNa5 treated screws. The NNa5 group was selected as it showed the best bacteriostatic inhibition efficiency among the other groups. The green zone indicates the area analysed for assessing BV/TV ratio. Fig. 11b, presenting the plot of the BV/TV (%) of the control and NNa5 after 4 weeks of implantation, indicates a slightly higher BV/TV ratio for the treated implants than the control. This implies that the initial degree of osseointegration of the NNa5 modified surface is better than that of the control. It can additionally be said that NNa5 has the potential to impart effective early osseointegration on further improvement of this technique.

Dual alkaline etching, combining NaOH and NH_4OH, is a new approach designed to give desired results at room temperature. It could provide benefits that are yet to be fully explored. Several studies on alkaline etching are mostly focused on either single alkaline etching or its combination with other electrolytes, hydroxyapatite (HA) coatings, SLA, and hydrothermal treatment.[39] For instance, Wu *et al.*[40] reported that alkaline etching can improve osseointegration and corrosion resistance by forming a highly bioactive surface compared to conventional acid etching methods. Toshiyuki *et al.*[41] compared the bone-bonding ability and bone-implant contact due to HA coating, and alkali heat treatment using rabbit models. This research reported that at 4, 8, and 16 weeks, the HA coated samples had higher bone-to-implant contact compared to alkali heat-treated ones. But at 8 and 16 weeks, alkali heat-treated samples showed more bone-bonding strength than the HA-coated ones. The untreated and HA-coated samples didn't show significant difference

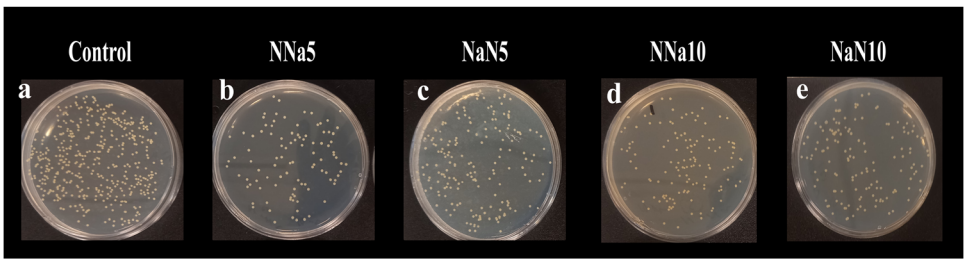

Fig. 9 Images of colonies formed by *S. aureus* on agar plates after direct contact test with: (a) control, (b) NNa5, (c) NNa10, (d) NaN5, and (e) NaN10.

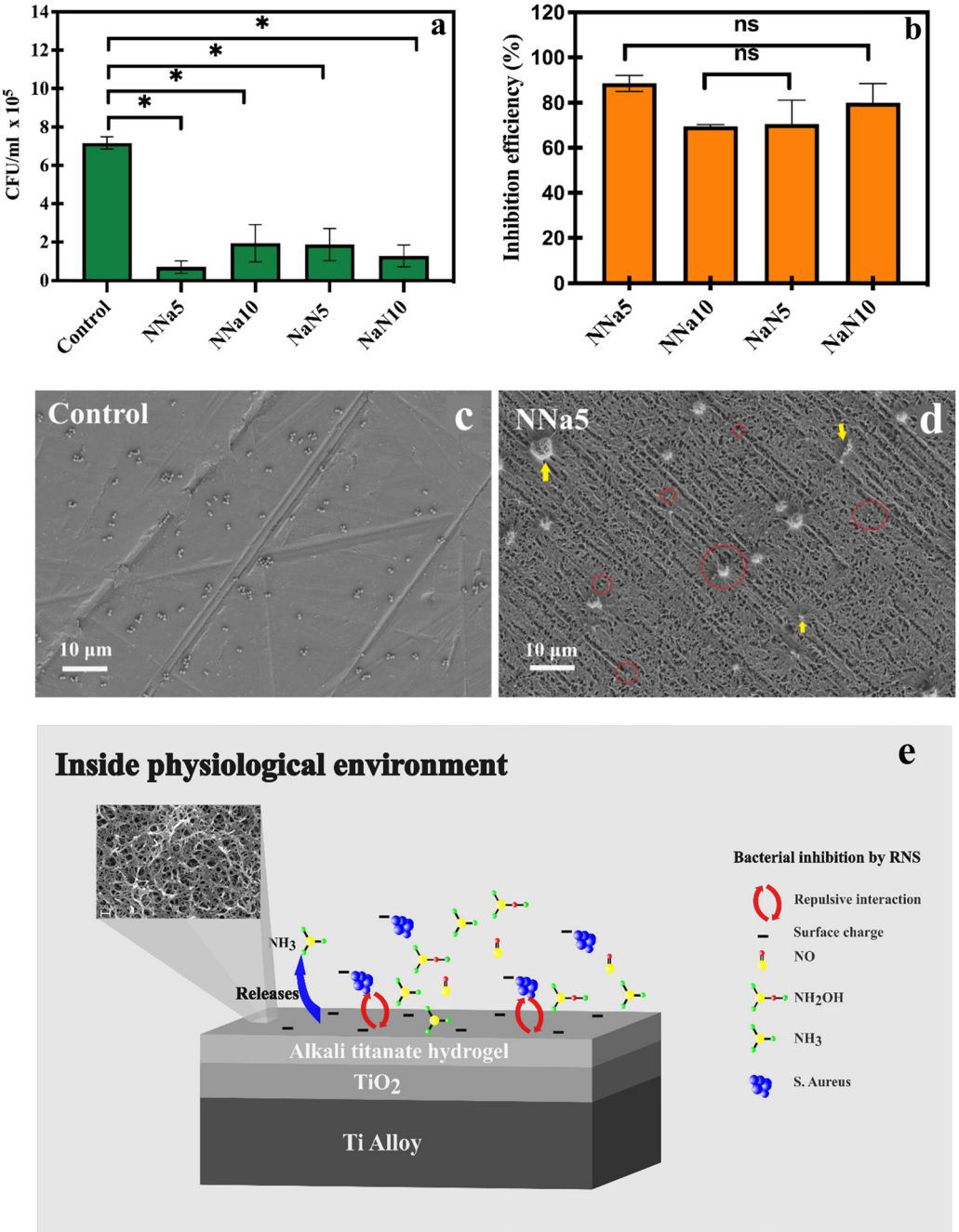

Fig. 10 (a) Colony forming units per ml (CFU per ml) measured after 1.5 hour *in vitro* incubation with *S. aureus* for the treated and untreated samples, (b) inhibition efficiency (%) of the dual alkaline etched samples, (c) and (d) SEM images of *S. aureus* on the control and NNa5, respectively, after 1.5 h of *in vitro* incubation. Yellow arrows represent etched residues and red rings engulf *S. aureus* on the etched surface. (e) Schematic representation of the inhibition action due to DAE surface treatment.

in bone-bonding strength, mostly due to the absorption of the HA layer, weakening its bond with the titanium substrate. Hence, they concluded that the bone-bonding strength and bone-to-implant contact on titanium implants can be effectively enhanced by alkali heat treatment. Additionally, after alkali heat treatment followed by vacuum storage for 52 weeks, the treated samples still exhibited good bioactivity.[42] A comparative *in vivo* study on machined and alkali-treated Ti alloy had also shown that the alkaline treatment can play a key role in improving osteoconduction.[43,44]

The primary difference and benefit of the dual alkaline etching used in this study is that it is performed at room temperature unlike other alkaline treatments, which involved at least low temperature heat treatment. It is easy to perform, independent of the shape of titanium, doesn't require expensive infrastructure, and has minimal effect on material composition and mechanical strength. It induces HA formation, bacteriostatic nature and compatibility. Hence, this simple dual alkali treatment could be utilized to achieve a good

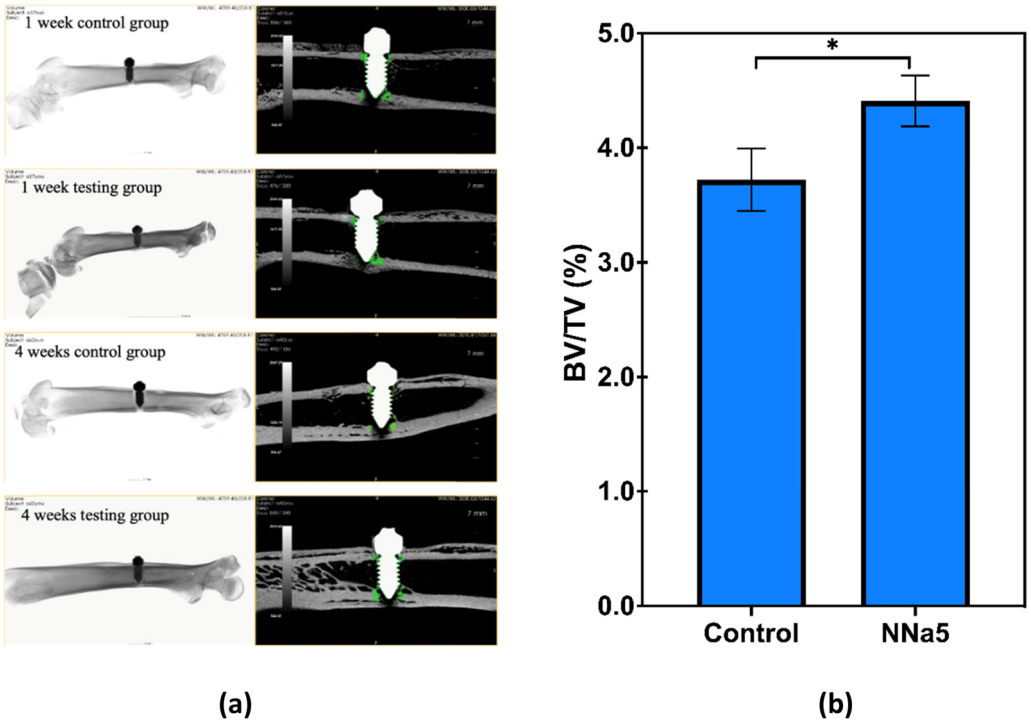

Fig. 11 (a) Micro-CT images of the control and test group (NNa5) after 1 week and 4 weeks of implantation in rat tibia; the green zone indicates the area of assessment used for BV/TV ratio. (b) Plot of BV/TV (%) in the control and test groups after 4 weeks of implantation.

bone-implant bonding, essential for a successful and stable implantation.

4. Conclusions

A room temperature dual alkaline surface modification technique was performed on Ti-6Al-4V plates. It is a surface-driven technique that not only modifies surface topography but also alters surface chemistry unlike SLA. The formation of a nanoporous network-like structure on the surface resulted in increased surface roughness and hydrophilicity. Antibacterial assessment showed that the treated surface, especially NNa5, exhibited 7 times greater bacterial inhibition than the control. Furthermore, all the modified surfaces showed apatite formation within a week's immersion time, implying that this treatment has the potential to promote rapid osseointegration on further optimization. Additionally, the *in vivo* studies also confirmed that NNa5-treated implants have better ability to osseointegrate compared to the control group. Thus, the dual alkaline etching performed at room temperature presents a promising strategy for implant surface modification, which promotes both bacterial inhibition and osseointegration on the titanium surface.

Author contributions

Conceptualization: W. Xia and H. Engqvist; methodology: S. Chettri, H. Zhou and W. Zhu performed the experiments. S. Chettri, H. Zhou, W. Xia and W. Zhu analysed the data. W. Xia, D. Seetharaman (remotely) discussed and supervised the project. S. Chettri, D. Seetharaman and W. Xia wrote the manuscript. W. Xia, D. Seetharaman reviewed and edited the manuscript. H. Engqvist, W. Xia and D. Seetharaman acquired financial support for the project.

Data availability

The authors declare that all data supporting the results reported in this study are available within the article (also available here, DOI: **https://doi.org/10.17632/np8f5wkt4f.1**). Additional data used for the study are available from the corresponding authors upon reasonable request.

Conflicts of interest

There are no conflicts to declare.

Acknowledgements

This work was financially supported by the Swedish Research Council (VR, 2021-05626), and UU Innovation (EFP). We also extend our gratitude to Myfab Uppsala for providing facilities and experimental support (Swedish Research Council, 2019-00207). Two of the authors acknowledge the Central Research Instruments Facility (CRIF), Prasanthi Nilayam, India, for providing the facilities to carry out this work.

References

1 J. W. Nicholson, Titanium Alloys for Dental Implants: A Review, *Prosthesis*, 2020, **2**(2), 100–116, DOI: **10.3390/prosthesis2020011**.

2 C. N. Elias, D. J. Fernandes, F. M. Souza, E. D. S. de, Monteiro and R. S. de Biasi, Mechanical and clinical properties of titanium and titanium-based alloys (Ti G2, Ti G4 cold worked nanostructured and Ti G5) for biomedical applications, *J. Mater. Res. Technol.*, 2019, **8**(1), 1060–1069, DOI: **10.1016/j.jmrt.2018.07.016**.

3 F. Accioni, J. Vázquez, M. Merinero, B. Begines and A. Alcudia, Latest Trends in Surface Modification for Dental Implantology: Innovative Developments and Analytical Applications, *Pharmaceutics*, 2022, **14**(2), 455, DOI: **10.3390/pharmaceutics14020455**.

4 D. Buser, S. F. M. Janner, J. G. Wittneben, U. Brägger, C. A. Ramseier and G. E. Salvi, 10-Year Survival and Success Rates of 511 Titanium Implants with a Sandblasted and Acid-Etched Surface: A Retrospective Study in 303 Partially Edentulous Patients, *Clin. Implant Dent. Relat. Res.*, 2012, **14**(6), 839–851, DOI: **10.1111/J.1708-8208.2012.00456.X**.

5 F. Husain, S. Gupta, S. Sood, N. Bhaskar and A. Jain, To evaluate the effect of anodized dental implant surface on cumulative implant survival and success. A systematic review and meta-analysis, *J. Indian Soc. Periodontol.*, 2022, **26**(6), 525–532, DOI: **10.4103/jisp.jisp_797_20**.

6 Z. Ur Rahman, I. Shabib and W. Haider, Surface characterization and cytotoxicity analysis of plasma sprayed coatings on titanium alloys, *Mater. Sci. Eng., C*, 2016, **67**, 675–683, DOI: **10.1016/j.msec.2016.05.070**.

7 J. B. Nebe, L. Müller, F. Lü, A. Ewald, C. Bergemann, E. Conforto and F. A. Mü Ller, Osteoblast response to biomimetically altered titanium surfaces, *Acta Biomater.*, 2008, **4**(6), 1985–1995, DOI: **10.1016/j.actbio.2008.05.028**.

8 H.-M. Kim, F. Miyaji, T. Kokubo, T. Nakamura and J. Wiley, Preparation of bioactive Ti and its alloys via simple chemical surface treatment, *J. Biomed. Mater. Res.*, 1996, **32**(3), 409–417, DOI: **10.1002/(SICI)1097-4636(199611)32:3**.

9 M.-S. Howe, W. Keys and D. Richards, Long-term (10-year) dental implant survival: A systematic review and sensitivity meta-analysis, *J. Dent.*, 2019, **84**, 9–21, DOI: **10.1016/j.jdent.2019.03.008**.

10 B. R. Chrcanovic, T. Albrektsson and A. Wennerberg, Reasons for failures of oral implants, *J. Oral Rehabil.*, 2014, **41**(6), 443–476, DOI: **10.1111/joor.12157**.

11 R. A. Abdelrahim, N. A. Badr and K. Baroudi, Effect of anodization and alkali-heat treatment on the bioactivity of titanium implant material (an in vitro study), *J. Int. Soc. Prev. Community Dent.*, 2016, **6**(3), 189–195, DOI: **10.4103/2231-0762.183107**.

12 T. C. Silva, L. M. Cardoso, T. N. Pansani, E. Alfredo, C. Souza-Costa and F. G. Basso, Effect Of Different Alkaline Treatments of Titanium Surface on Human Osteoblasts Metabolism, *Braz. Dent. J.*, 2024, **35**, e245786, DOI: **10.1590/0103-6440202405786**.

13 I. M. Hamouda, E. T. Enan, E. E. Al-Wakeel and M. K. Yousef, Alkali and heat treatment of titanium implant material for bioactivity, *Int. J. Oral Maxillofac. Implants*, 2012, **27**(4), 776–784.

14 M. Wei, H.-M. Kim, T. Kokubo and J. H. Evans, Optimizing the bioactivity of alkaline-treated titanium alloy, *Mater. Sci. Eng., C*, 2002, **20**(1–2), 125–134, DOI: **10.1016/S0928-4931(02)00022-X**.

15 O. Janson, S. Gururaj, S. Pujari-Palmer, M. Karlsson Ott, M. Strømme, H. Engqvist and K. Welch, Titanium surface modification to enhance antibacterial and bioactive properties while retaining biocompatibility, *Mater. Sci. Eng., C*, 2019, **96**, 272–279, DOI: **10.1016/j.msec.2018.11.021**.

16 T. Kokubo and S. Yamaguchi, Novel bioactive materials developed by simulated body fluid evaluation: Surface-modified Ti metal and its alloys, *Acta Biomater.*, 2016, **44**, 16–30, DOI: **10.1016/j.actbio.2016.08.013**.

17 T. Kokubo and H. Takadama, How useful is SBF in predicting in vivo bone bioactivity, *Biomaterials*, 2006, **27**(15), 2907–2915, DOI: **10.1016/j.biomaterials.2006.01.017**.

18 I. Georgakopoulos-Soares, E. L. Papazoglou, P. Karmiris-Obratański, N. E. Karkalos and A. P. Markopoulos, Surface antibacterial properties enhanced through engineered textures and surface roughness: A review, *Colloids Surf., B*, 2023, **231**, 113584, DOI: **10.1016/j.colsurfb.2023.113584**.

19 N. Mitik-Dineva, J. Wang, R. C. Mocanasu, P. R. Stoddart, R. J. Crawford and E. P. Ivanova, Impact of nano-topography on bacterial attachment, *Biotechnol. J.*, 2008, **3**(4), 536–544, DOI: **10.1002/biot.200700244**.

20 S. L. R. Da Silva, L. O. Kerber, L. Amaral and C. A. Dos Santos, X-ray diffraction measurements of plasma-nitrided Ti–6Al–4V, *Surf. Coat. Technol.*, 1999, **116–119**, 342–346, DOI: **10.1016/S0257-8972(99)00204-2**.

21 K. Lee and D. Yoo, Large-area sodium titanate nanorods formed on titanium surface via NaOH alkali treatment, *Arch. Metall. Mater.*, 2015, **60**(2), 1371–1374, DOI: **10.1515/amm-2015-0133**.

22 H. M. Kim, F. Miyaji, T. Kokubo, S. Nishiguchi and T. Nakamura, Graded surface structure of bioactive titanium prepared by chemical treatment, *J. Biomed. Mater. Res.*, 1999, **45**(2), 100–107, DOI: **10.1002/(sici)1097-4636(199905)45:2<100::aid-jbm4>3.0.co;2-0**.

23 A. Trenczek-Zajac, M. Radecka, K. Zakrzewska, A. Brudnik, E. Kusior, S. Bourgeois, M. C. M. de Lucas and L. Imhoff, Structural and electrical properties of magnetron sputtered Ti (ON) thin films: The case of TiN doped in situ with oxygen, *J. Power Sources*, 2009, **194**(1), 93–103, DOI: **10.1016/j.jpowsour.2008.12.112**.

24 J.-C. Hsu, Y.-H. Lin and P. Wang, X-ray Photoelectron Spectroscopy Analysis of Nitrogen-Doped TiO_2 Films Prepared by Reactive-Ion-Beam Sputtering with Various NH_3/O_2 Gas Mixture Ratios, *Coatings*, 2020, **10**, 47, DOI: **10.3390/coatings10010047**.

25 X. P. S. Database (SRD 20), *Version 5*, National Institute of Standards and Technology (NIST), U.S. Department of Commerce, **https://srdata.nist.gov/xps/ElmComposition**.

26 H. Takadama, H.-M. Kim, T. Kokubo and T. Nakamura, XPS Study of the Process of Apatite Formation on Bioactive Ti–6Al–4V Alloy in Simulated Body Fluid, *Sci. Technol. Adv. Mater.*, 2001, **2**, 389–396, DOI: **10.1016/S1468-6996(01)00007-9**.

27 H. M. Kim, F. Miyaji, T. Kokubo and T. Nakamura, Apatite-forming ability of alkali-treated Ti metal in body environment, *J. Ceram. Soc. Jpn.*, 1997, **105**(1218), 111–116, DOI: **10.2109/jcersj.105.111**.

28 W. A. Camargo, S. Takemoto, J. W. Hoekstra, S. C. G. Leeuwenburgh, J. A. Jansen, J. J. J. P. Van Den Beucken and H. S. Alghamdi, Effect of surface alkali-based treatment of titanium implants on ability to promote in vitro mineralization and in vivo bone formation, *Acta Biomater.*, 2017, **57**, 511–523, DOI: **10.1016/j.actbio.2017.05.016**.

29 H. L. Siew, M. H. Qiao, C. H. Chew, K. F. Mok, L. Chan and G. Q. Xu, Adsorption and reaction of NH3 on Ti/Si(1 0 0), *Appl. Surf. Sci.*, 2001, **173**(1–2), 95–102, DOI: **10.1016/s0169-4332(00)00896-5**.

30 H. M. Kim, F. Miyaji and T. Kokubo, *et al.*, Effect of heat treatment on apatite-forming ability of Ti metal induced by alkali treatment, *J. Mater. Sci.: Mater. Med.*, 1997, **8**, 341–347, DOI: **10.1023/A:1018524731409**.

31 M. W. Hussain, S. S. Abullais, T. A. Naqash and M. Y. S. Bhat, Microbial Etiology and Antimicrobial Therapy of Peri-implantitis: A Comprehensive Review, *Open Dent. J.*, 2018, **12**(1), 1113–1122, DOI: **10.2174/1874210601812011113**.

32 G. E. Salvi, M. M. Fürst, N. P. Lang and G. R. Persson, One-year bacterial colonization patterns of Staphylococcus aureus and other bacteria at implants and adjacent teeth, *Clin. Oral. Implants Res.*, 2008, **19**(3), 242–248, DOI: **10.1111/j.1600-0501.2007.01470.x**.

33 S. Rokadiya and N. Malden, An implant periapical lesion leading to acute osteomyelitis with isolation of Staphylococcus aureus, *British Dental Journal*, 2008, **205**, 489–491, DOI: **10.1038/sj.bdj.2008.935**.

34 H. Zhou, C. Persson, O. Donzel-Gargand, H. Engqvist and W. Xia, Structural Si3N4-SiO2 glass ceramics with bioactive and anti-bacterial properties, *J. Eur. Ceram. Soc.*, 2024, **44**(6), 4260–4271, DOI: **10.1016/j.jeurceramsoc.2024.01.016**.

35 L. Li, J. Gao, G. Chang, J. Mu, E. Xu, X. Liu, J. Yan, H. Zhou and L. Zhang, Effect of β-SiAlON content on the sintering and bacteriostatic properties of β-SiAlON–Si3N4 composite ceramics, *Ceram. Int.*, 2022, **48**(22), 33704–33711, DOI: **10.1016/j.ceramint.2022.07.316**.

36 G. Pezzotti, A spontaneous solid-state NO donor to fight antibiotic resistant bacteria, *Mater. Today Chem.*, 2018, **9**, 80–90, DOI: **10.1016/j.mtchem.2018.05.004**.

37 S. Roessler, R. Zimmermann, D. Scharnweber, C. Werner and H. Worch, Characterization of oxide layers on Ti6Al4V and titanium by streaming potential and streaming current measurements, *Colloids Surf., B*, 2002, **26**(4), 387–395, DOI: **10.1016/S0927-7765(02)00025-5**.

38 A. V. Singh, V. Vyas, R. Patil, V. Sharma, P. E. Scopelliti, G. Bongiorno, A. Podestà, C. Lenardi, W. N. Gade and P. Milani, Quantitative Characterization of the Influence of the Nanoscale Morphology of Nanostructured Surfaces on Bacterial Adhesion and Biofilm Formation, *PLoS One*, 2011, **6**(9), e25029, DOI: **10.1371/journal.pone.0025029**.

39 J. Li, G. Wang, D. Wang, Q. Wu, X. Jiang and X. Liu, Alkali-treated titanium selectively regulating biological behaviors of bacteria, cancer cells and mesenchymal stem cells, *J. Colloid Interface Sci.*, 2014, **436**, 160–170, DOI: **10.1016/j.jcis.2014.08.053**.

40 Y. Wu, K. Wan, J. Lu, C. Yuan, Y. Cui, R. Duan and J. Yu, Research Progress on Surface Modification of Titanium Implants, *Coatings*, 2025, **15**(2), 229, DOI: **10.3390/coatings15020229**.

41 T. Kawai, M. Takemoto, S. Fujibayashi, M. Tanaka, H. Akiyama, T. Nakamura and S. Matsuda, Comparison between alkali heat treatment and sprayed hydroxyapatite coating on thermally-sprayed rough Ti surface in rabbit model: Effects on bone-bonding ability and osteoconductivity, *J. Biomed. Mater. Res., Part B*, 2015, **103**(5), 1069–1081, DOI: **10.1002/jbm.b.33281**.

42 M. Kamo, M. Kyomoto and F. Miyaji, Time course of surface characteristics of alkali- and heat-treated titanium dental implants during vacuum storage, *J. Biomed. Mater. Res., Part B*, 2017, **105**, 1453–1460, DOI: **10.1002/jbm.b.33686**.

43 X. Lu, Y. Leng, X. Zhang, J. Xu, L. Qin and C. Chan, Comparative study of osteoconduction on micromachined and alkali-treated titanium alloy surfaces in vitro and in vivo, *Biomaterials*, 2005, **26**(14), 1793–1801, DOI: **10.1016/j.biomaterials.2004.06.009**.

44 Y. Okuzu, S. Fujibayashi, S. Yamaguchi, K. Yamamoto, T. Shimizu, T. Sono, K. Goto, B. Otsuki, T. Matsushita and T. Kokubo, *et al.*, Strontium and magnesium ions released from bioactive titanium metal promote early bone bonding in a rabbit implant model, *Acta Biomater.*, 2017, **63**, 383–392, DOI: **10.1016/j.actbio.2017.09.019**.